

# Metallomics

Accepted Manuscript



This is an *Accepted Manuscript*, which has been through the Royal Society of Chemistry peer review process and has been accepted for publication.

*Accepted Manuscripts* are published online shortly after acceptance, before technical editing, formatting and proof reading. Using this free service, authors can make their results available to the community, in citable form, before we publish the edited article. We will replace this *Accepted Manuscript* with the edited and formatted *Advance Article* as soon as it is available.

You can find more information about *Accepted Manuscripts* in the [Information for Authors](#).

Please note that technical editing may introduce minor changes to the text and/or graphics, which may alter content. The journal's standard [Terms & Conditions](#) and the [Ethical guidelines](#) still apply. In no event shall the Royal Society of Chemistry be held responsible for any errors or omissions in this *Accepted Manuscript* or any consequences arising from the use of any information it contains.

1  
2  
3 **Kinetic Results for Mutations of Conserved Residues H304 and R309 of Human**  
4 **Sulfite Oxidase Point to Mechanistic Complexities**  
5  
6

7  
8 **Amanda C. Davis,<sup>1</sup> Kayunta Johnson-Winters,<sup>2\*</sup> Anna R. Arnold,<sup>1</sup> Gordon Tollin,<sup>1</sup>**  
9

10 **John H. Enemark<sup>1</sup>**  
11

12 <sup>1</sup>Department of Chemistry and Biochemistry, University of Arizona, Tucson, Arizona,  
13  
14 85721-0041  
15

16  
17 <sup>2</sup>Department of Chemistry and Biochemistry, University of Texas at Arlington, Arlington,  
18  
19 Texas 76019-0065  
20

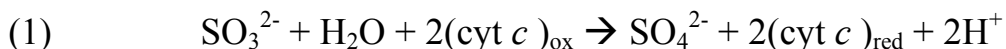
21 *\*Kayunta@uta.edu*  
22  
23  
24  
25  
26  
27  
28  
29  
30  
31  
32  
33  
34  
35  
36  
37  
38  
39  
40  
41  
42  
43  
44  
45  
46  
47  
48  
49  
50  
51  
52  
53  
54  
55  
56  
57  
58  
59  
60

**Abstract**

Several point mutations in the gene of human sulfite oxidase (hSO) result in isolated sulfite oxidase deficiency, an inherited metabolic disorder. Three conserved residues (H304, R309, K322) are hydrogen bonded to the phosphate group of the molybdenum cofactor, and the R309H and K322R mutations are responsible for isolated sulfite oxidase deficiency. The kinetic effects of the K322R mutation have been previously reported (Rajapakshe et al. 2012, *Chem. Biodiversity* 9, 1621-1634); here we investigate several mutants of H304 and R309 by steady-state kinetics, laser flash photolysis studies of intramolecular electron transfer (IET), and spectroelectrochemistry. An unexpected result is that all of the mutants show *decreased* rates of IET but *increased* steady-state rates of catalysis. However, in all cases the rate of IET is greater than the overall turnover rate, showing that IET is not the rate determining step for any of the mutations.

## Introduction

Sulfite oxidizing enzymes are molybdenum-containing enzymes that occur in animals, plants and bacteria. In animals, sulfite oxidase (SO) is a molybdoheme enzyme that is located in the intermembrane space of the mitochondria and is essential for oxidizing toxic sulfite to sulfate, which can then be excreted (eq. 1). The proposed catalytic cycle for human sulfite oxidase (hSO) is shown in Figure 1. Regeneration of the enzyme includes two, one-electron *intramolecular* electron transfers (IET) from the molybdenum (Mo) to the heme Fe and two, one-electron *intermolecular* electron transfers from the Fe to external ferricytochrome *c* (1-5).



In humans, sulfite oxidase deficiency is an inherited metabolic disorder that leads to severe neonatal neurological defects and early death (6). The inability to biosynthesize the molybdenum cofactor (Moco, Figure 2) results in “general sulfite oxidase deficiency”, which compromises all molybdenum enzymes (7). However, recent determination of the biosynthetic pathway of Moco has made possible the first clinical treatment of “general SO deficiency” (8). Several point mutations in the hSO gene also result in sulfite oxidase deficiency (9, 10). Our research has focused on investigating the effects of such point mutations on the structure, solution dynamics, and the catalytic mechanism of hSO with the long-term goal that understanding “isolated sulfite oxidase deficiency” at the molecular level may eventually lead to treatment protocols for this condition.

1  
2  
3  
4  
5  
6  
7  
8  
9  
10  
11  
12  
13  
14  
15  
16  
17  
18  
19  
20  
21  
22  
23  
24  
25  
26  
27  
28  
29  
30  
31  
32  
33  
34  
35  
36  
37  
38  
39  
40  
41  
42  
43  
44  
45  
46  
47  
48  
49  
50  
51  
52  
53  
54  
55  
56  
57  
58  
59  
60

No crystal structure is available for hSO, so the crystal structure of the highly homologous chicken sulfite oxidase (cSO), shown in Figure 3, is used as a structural template for hSO (11). The crystal structure of cSO shows that the enzyme is a homodimer and that each monomer is made up of a molybdenum cofactor (Moco) containing domain and a smaller, cytochrome *b*<sub>5</sub>-type domain (heme domain). These two domains are linked by a flexible polypeptide tether with no secondary structure (11). In the crystal structure and in frozen solution (12) the Mo···Fe distance is ~32 Å. However, it is proposed that in fluid solution the tether allows the heme domain to move within close proximity to the Mo center so that rapid IET and efficient catalysis can occur (12-16).

Previous studies of hSO mutants have shown a range of interesting properties and reactivities, some of which were quite unexpected. These mutations include: deletion of tether residues (17); mutation of the aromatic residues around both the heme and Mo domains (18, 19); mutation of conserved active site residues (20-22); and producing some of the fatal mutations (22-26) such as R160Q and K322R. Although many of these mutants have provided much insight into the structural and kinetic characteristics of hSO, some have shown unexplained or even paradoxical results. For example, mutation of H337 and W338 on the surface of the Mo domain influence the potential of the heme domain, despite the large distance between these residues and the heme in the crystal structure (18). Mutations such as K322R, W338A, H337R, and ΔKVATV, show IET rates that are much less than wt hSO and sometimes less their own  $k_{\text{cat}}$  values, while  $k_{\text{cat}}$  in many cases has *increased* significantly as compared to wt (17, 18, 25). These results illustrate the complexity of hSO and indicate that the roles of conformational change and

1  
2  
3 other factors in the catalytic cycle and IET reactions of hSO and their relationship to  
4  
5 isolated sulfite oxidase deficiency are yet to be understood.  
6  
7

8 The phosphate group of the molybdenum cofactor is associated with three  
9  
10 conserved, positively charged residues, H304, R309, and K322, that hydrogen bond to  
11  
12 one another and to the negatively charged phosphate group (Figure 2) (11). Two of these  
13  
14 residues, R309H and K322R, have been linked to isolated sulfite oxidase deficiency (10).  
15  
16 A study of the K322R mutant has been recently described (25); the present study focuses  
17  
18 on histidine 304 (H304) and arginine 309 (R309). H304 is located on the surface of the  
19  
20 Mo domain and is hydrogen bonded to R309 and to the phosphate group of Moco. R309  
21  
22 is located just under the surface of the Mo domain and hydrogen bonds to the phosphate  
23  
24 of Moco, H304, and K322 (11). In the present study, several mutations of H304 and  
25  
26 R309 have been prepared and purified, and the recombinant enzymes have been  
27  
28 characterized using steady-state kinetics, laser flash photolysis, and  
29  
30 spectroelectrochemistry. The unexpected results that were obtained for the H304 and  
31  
32 R309 mutants are compared to the other classes of hSO mutants described above, and the  
33  
34 challenges of developing a comprehensive molecular mechanism for catalysis by hSO are  
35  
36 discussed.  
37  
38  
39  
40  
41  
42  
43  
44  
45

## 46 **Experimental**

### 47 **Site-directed mutagenesis**

48  
49 The mutations were introduced into the pTG918 plasmid containing the wt hSO  
50  
51 sequence using the Quick Change Site-Directed Mutagenesis protocol (Stratagene) (27).  
52  
53  
54

55 The Sequetech Corporation DNA analysis facility in Mountain View, California  
56  
57  
58  
59  
60

1  
2  
3 confirmed each of the single amino acid mutations by DNA sequence analysis (see  
4 supporting information, Table S1).  
5  
6

### 7 8 **Protein over-expression and purification** 9

10 The recombinant hSO mutants were introduced into *E. coli* and purified using a  
11 previously established method for hSO proteins with the following modifications (27, 28).  
12 After the DE-52 column (GE Healthcare), the fractions with an  $A_{413}/A_{280}$  ratio of 0.80 or  
13 greater were collected and purified further through a Phenyl Sepharose column (GE  
14 Healthcare). The fractions that had an  $A_{413}/A_{280}$  ratio of 0.95 or greater were then purified  
15 using a Superdex 200 column (GE Healthcare). The enzyme concentration was calculated  
16 by using the molar extinction coefficient of  $113,000 \text{ M}^{-1} \text{ cm}^{-1}$  at 413 nm (20). The Mo:Fe  
17 ratio of each purified protein was determined using an IRIS Advantage Inductively  
18 Coupled Plasma Emission Spectrometer (*ICP-OES*) from the Jarrell Ash Corporation (see  
19 supporting information, Table S2).  
20  
21  
22  
23  
24  
25  
26  
27  
28  
29  
30  
31  
32  
33

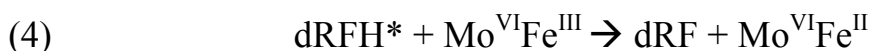
### 34 **Steady-state kinetics** 35

36 Steady-state kinetics studies were performed aerobically at 25°C using a Varian  
37 Cary-300 spectrophotometer. Initial velocities were calculated following the reduction of  
38 freshly prepared oxidized cyt *c* (horse heart, Sigma) at 550 nm ( $\epsilon = 19,630 \text{ M}^{-1} \text{ cm}^{-1}$ )  
39 (29). Samples were prepared using 20 mM Tris buffer, adjusted to pH 7.6 using acetic  
40 acid. 20 mM Bis-Tris was used for samples for which the pH was adjusted to 6.8 using  
41 acetic acid. The kinetic profile for obtaining the Michaelis-Menten constant,  $K_m$ , for  
42 sulfite and  $k_{\text{cat}}$ , for the reduction of cyt *c*, was studied using a saturating concentration of  
43 cyt *c* (400  $\mu\text{M}$ ; 10-fold greater than  $K_m^{\text{cyt } c}$  for wt hSO) and by varying the concentration  
44 of sulfite between 1  $\mu\text{M}$  and 400  $\mu\text{M}$ . The concentration of enzyme was 50 nM. A  
45  
46  
47  
48  
49  
50  
51  
52  
53  
54  
55  
56  
57  
58  
59  
60

sample kinetic profile is shown in the Supporting Information. Since  $k_{\text{cat}}$  is defined as per cyt  $c$  reduced (29) and two cyt  $c$  are reduced per turnover cycle (Figure 1),  $k_{\text{turnover}} = \frac{1}{2} k_{\text{cat}}$ . Table S3 summarizes the kinetic parameters for wt hSO and each of the mutants.

### Laser flash photolysis

IET 2 (Figure 1) in the hSO catalytic cycle can be studied using a photochemical one-electron reduction of the Fe(III) state and following its re-oxidation by Mo(VI) (30). Laser flash photolysis experiments of the mutants were done anaerobically using 300  $\mu\text{L}$  of solution containing  $\sim 90 \mu\text{M}$  5-deazariboflavin (dRF), 0.5 mM freshly prepared semicarbazide (the sacrificial reductant) and enzyme concentrations of 10  $\mu\text{M}$ , 15  $\mu\text{M}$ , and 20  $\mu\text{M}$ . The methodologies for determining equilibrium constants and rate constants for hSO using this technique have been described previously (13). The laser flash system (31) and the process by which the enzyme sample is photochemically reduced have also been previously described (32-34) and are summarized below (eqs. 2-5).





1  
2  
3  
4  
5  
6  
7  
8  
9  
10  
11  
12  
13  
14  
15  
16  
17  
18  
19  
20  
21  
22  
23  
24  
25  
26  
27  
28  
29  
30  
31  
32  
33  
34  
35  
36  
37  
38  
39  
40  
41  
42  
43  
44  
45  
46  
47  
48  
49  
50  
51  
52  
53  
54  
55  
56  
57  
58  
59  
60

By fitting the heme re-oxidation curve with an exponential function, the IET rate constant,  $k_{et}$ , can be calculated (eq. 6). The IET rate constant ( $k_{et}$ ) is the sum of the forward ( $k_f$ ) and the reverse ( $k_r$ ) electron transfer rate constants (eq. 7). The parameters  $a$  and  $b$  are determined from kinetic traces and can be used to calculate the equilibrium constant (eqs. 8-10). Note that the direction of IET in the laser flash photolysis experiments is actually the reverse of the net physiological catalytic reaction (Figure 1).

$$(6) \quad dA_{555}/dt = a + b \exp(-k_{et}t)$$

$$(7) \quad k_{et} = k_f + k_r$$

$$(8) \quad a = A_0 (k_r/k_{et})$$

$$(9) \quad b = A_0 (k_f/k_{et})$$

$$(10) \quad K_{eq} = k_f/k_r = b/a$$

### Spectroelectrochemistry

Spectroelectrochemical measurements of the heme reduction potentials were determined using the same type of instrumentation and reference electrode as described previously (35, 36). A spectroelectrochemical cell, gold working electrode, and platinum wire auxiliary electrode (BASi) were used to hold a 400  $\mu$ L sample. Protein samples were prepared in 20 mM Tris buffer, pH 7.4, containing two electrochemical mediators, hexaammineruthenium chloride and anthraquinone 2-sulfonate (purchased from Aldrich) (37). Protein concentration ranged from 300  $\mu$ M to 400  $\mu$ M.

Since the wavelength dependences of the extinction coefficients of the

1  
2  
3 reduced and oxidized forms of hSO differ from one another, the ratio of the oxidized to  
4 reduced forms is directly related to the absorbances of the optical spectra via Beer's law,  
5  
6 and the change in absorbance with respect to the applied potential can be fit to the Nernst  
7  
8 equation (Eq. 11) using the nonlinear-least-squares fitting algorithm in the software  
9  
10 program Origin<sup>®</sup>:  
11  
12  
13

$$(11) \quad E_{app} = E^0 + 2.303(RT/nF)\log_{10}([Ox]/[Red])$$

14  
15  
16  
17  
18 where  $E_{app}$  is the applied potential,  $E_0$  is the midpoint potential determined from these  
19  
20 data, and [Ox] and [Red] are, respectively, the concentrations of the Fe(III) and Fe(II)  
21  
22 states of the  $b_5$  heme of hSO. For a previous application of this method to hSO see  
23  
24 Figure 4 of ref 17.  
25  
26  
27  
28

## 29 Results and discussion

### 30 **Steady-state kinetics**

31  
32  
33  
34  
35 The diversity of amino acids in the eight various mutations of H304 and R309  
36 described herein involve replacing the histidine or arginine with a residue of different  
37 charge or of a drastically different size. All of the H304 and R309 mutations had *greater*  
38 catalytic activity than wt hSO. For H304A and H304E,  $k_{cat}$  was doubled compared to wt  
39 hSO, and all of the other mutant enzymes were three to four times as fast as wt hSO.  
40  
41 Surprisingly, R309E, a mutation in which a positively charged residue is changed to a  
42 negatively charged residue, showed the highest  $k_{cat}$  of all the mutants. The increases in  
43  
44  $k_{cat}$  for all the mutants, rather than significant decreases, were unexpected given the  
45  
46 hydrogen bonding interactions of H304 and R309 with the phosphate group of the  
47  
48 molybdenum cofactor and the proximity of these residues to the active site of the enzyme.  
49  
50  
51  
52  
53  
54  
55  
56  
57  
58  
59  
60

1  
2  
3 On the other hand, the fact that H304 and R309 are conserved across all eukaryotic sulfite  
4 oxidases suggests that their primary role may be anchoring or stabilizing Moco through  
5  
6 oxidases suggests that their primary role may be anchoring or stabilizing Moco through  
7  
8 hydrogen bonding rather than optimizing catalytic activity. Crystal structures of  
9  
10 appropriate mutants of H304 and R309 are required to test this hypothesis.

11  
12 The  $K_m^{\text{sulfite}}$  values for the H304 and R309 mutant enzymes were not drastically  
13 altered from wt hSO, despite the fact that H304 and R309 are located within relatively  
14 close proximity to the Mo active site. H304F, H304E, R309K, and R309M showed  $K_m$   
15 values similar to wt, whereas H304R, R309H, and the double mutant version of the two,  
16  
17 H304R/R309H, showed slight increases in  $K_m^{\text{sulfite}}$ . R309E, which showed the greatest  
18 increase in activity, also showed the greatest increase in  $K_m$ . So although this mutation  
19 caused the enzyme to catalyze the oxidation of sulfite to sulfate much more quickly than  
20 wt, it did not bind sulfite as efficiently as wt hSO. Lastly, H304A, a mutation that  
21 removes the charge, hydrogen bonding, and is of smaller size, showed a decrease in  
22  
23  $K_m^{\text{sulfite}}$ , thus binding sulfite more efficiently than wt. Again,  $k_{cat}$  was increased compared  
24 to wt.  
25  
26

### 27 28 29 30 31 32 33 34 35 36 37 38 39 **Intramolecular electron transfer (IET)**

40  
41 All of the R309 mutations caused large decreases in the  $k_{et}$  value for IET that were  
42 pH dependent (Figure 5B). R309K showed the least change, and R309E showed the most  
43 change. This makes sense in that mutating the arginine to lysine (R309K) keeps the  
44 positive charge and has the most comparable size to wt of all the mutations. Mutating the  
45 arginine to glutamate (R309E) changes the charge from positive to negative while  
46  
47 reducing the size of the residue. The result for R309E is also consistent with the proposal  
48 that the rate-limiting step of IET is a docking process, in which the negatively charged  
49  
50  
51  
52  
53  
54  
55  
56  
57  
58  
59  
60

1  
2  
3 heme domain interacts with the positively charged Mo domain (38). Decreasing the  
4  
5 positive charge of the Mo domain by the R309E mutation should decrease the  
6  
7 electrostatic attraction between the two domains and thereby decrease the IET rate.  
8  
9

10 At pH 7.6 and 6.8, the IET rates of R309K, R309H, and R309M were  
11  
12 approximately half that of wt hSO (Figure 5B). For all three of these mutants,  $k_{\text{et}} > \frac{1}{2} k_{\text{cat}}$   
13  
14 =  $k_{\text{turnover}}$ , indicating that IET 2 is not the rate determining step. At pH 7.6, R309E  
15  
16 showed the smallest  $k_{\text{et}}$  ( $67 \text{ s}^{-1}$ ) of the R309 mutants, but even this mutant with reversed  
17  
18 charges had  $k_{\text{et}}$  slightly larger than  $k_{\text{turnover}}$  ( $63 \text{ s}^{-1}$ , Table S3). At pH 6.8 R309E did not  
19  
20 show any reoxidation of the Fe(II).  
21  
22  
23

24 The IET rates of the H304 mutants are shown in Figure 5A. At pH 7.4, the IET  
25  
26 rates of H304A, H304F, and H304R/R309H were less than half as fast as wt, and H304E  
27  
28 and H304R were about  $100 \text{ s}^{-1}$  slower than wt hSO. At pH 6.8, all mutant enzymes had  
29  
30 IET rates that were two to three times less than that of wt hSO, with H304F being the  
31  
32 most affected.  
33  
34  
35

36 It is interesting to note that the IET rates *decreased* significantly, while the rates  
37  
38 of catalysis *increased* considerably. This apparent discrepancy has previously been  
39  
40 explained for other hSO mutants by the possible differences in the enzyme starting  
41  
42 conformations that are probed by the steady-state kinetics and laser flash photolysis  
43  
44 experiments (18). During steady-state kinetics, the proposed first step (Figure 1) is the  
45  
46 binding of sulfite and a two-electron reduction of the Mo(VI)/Fe(III) resting state species  
47  
48 to Mo(IV)/Fe(III). The first IET reaction (IET 1, Figure 1) converts Mo(IV)/Fe(III) to  
49  
50 Mo(V)/Fe(II). This results in the appearance of a Mo(V) EPR signal and is known to  
51  
52 occur in all hSO mutants, even the fatal R160Q mutant (24). From previous  
53  
54  
55  
56  
57  
58  
59  
60

1  
2  
3 microcoulometry studies of cSO, the IET 1 step should have a driving force of ~300 mV  
4 (39). The second IET step of the proposed catalytic cycle (IET 2) occurs after transfer of  
5  
6 an electron to exogenous cyt *c*. Thus, in the forward reaction of the overall catalytic cycle,  
7  
8 the IET 2 step is initiated from the *one-electron reduced* Mo(V)/Fe(III) state of the  
9  
10 enzyme, and both the sulfite and cyt *c* substrates are present. In contrast, the laser flash  
11  
12 photolysis determination of IET 2 starts with the fully oxidized resting state  
13  
14 (Mo(VI)/Fe(III)) of the enzyme and no substrates are present. One-electron  
15  
16 photoreduction of this oxidized resting state species gives Mo(VI)/Fe(II), and the  
17  
18 postulated conformational equilibria of this one-electron reduced state enables IET 2 to  
19  
20 be observed in the forward and reverse directions (eq. 5) (13). The R309 and H304  
21  
22 mutations that show large decreases in IET 2 rates (Figure 5) but high  $k_{\text{cat}}$  values (Figure  
23  
24 4A) may reflect unfavorable resting state conformations of the fully oxidized enzymes,  
25  
26 slow motional dynamics for bringing the heme and molybdenum domains into close  
27  
28 proximity for the IET 2 reaction after photoreduction, or altered Mo(VI/V) potentials that  
29  
30 make  $k_f$  (eq. 5) thermodynamically unfavorable in the flash photolysis experiments. The  
31  
32 reduction potentials of the metal centers are discussed in the following section.  
33  
34  
35  
36  
37  
38  
39

### 40 **Spectroelectrochemistry and IET equilibrium constants**

41  
42  
43 H304 and R309 are located in the Mo domain, and it seems reasonable to suppose  
44  
45 that unless the heme domain comes within close proximity of them during the IET  
46  
47 conformational change, these residues should not influence the heme midpoint potential  
48  
49 because of their large distance from the iron. Due to a limited supply of protein,  
50  
51 spectroelectrochemistry could not be performed on two mutant hSO enzymes, H304A  
52  
53  
54  
55  
56  
57  
58  
59  
60

1  
2  
3 and R309E. However, the remaining mutations showed a variety of effects on the heme  
4  
5 midpoint potential.  
6

7  
8 The H304E, H304R, and H304R/R309H had heme potentials similar to that of wt  
9  
10 hSO (54 mV). H304F hSO showed the largest change of the H304 mutations with an 11  
11  
12 mV negative shift. Overall, however, the H304 mutations had only small effects on the  
13  
14 heme midpoint potential.  
15  
16

17  
18 Two R309 mutations, R309K and R309M, caused significant decreases in the  
19  
20 heme midpoint potential, with changes of -31 mV and -24 mV, respectively. In contrast,  
21  
22 R309H hSO had a heme potential close to that of wt.  
23

24  
25 The spectroelectrochemistry results suggest that the heme domain interacts with  
26  
27 the surface of the Mo domain near H304 and R309. This is supported by the changes in  
28  
29 heme midpoint potential of R309M, R309K, and H304F and the dramatic changes in  
30  
31 their IET 2 rates. The docking position of the heme during IET 2 is still unknown, but it  
32  
33 has been proposed that the negatively charged heme domain interacts with the positively  
34  
35 charged active site, possibly hydrogen bonding to active site residue R160 (40). During  
36  
37 catalysis, however, having sulfite binding and sulfate release happening almost  
38  
39 simultaneously with the heme domain docking may be unfavorable. An alternative model  
40  
41 is that the heme docks in another location on the surface of the Mo domain that is close to  
42  
43 the active site (18), such as the H304R, R309 area. Under this hypothesis the IET 2 rates  
44  
45 and the heme potential would be altered if this interaction were disrupted by mutation of  
46  
47 H304 or R309.  
48  
49  
50  
51

52  
53 The potentials for the Mo center cannot be measured directly by  
54  
55 spectroelectrochemistry, which is dominated by the absorbance of the heme. Insufficient  
56  
57  
58  
59  
60

1  
2  
3 amounts of the mutant proteins were available to measure the Mo potentials by EPR  
4  
5 titrations. However, the Mo(VI/V) potentials can be calculated from the IET equilibrium  
6  
7 constants from the flash photolysis experiments (eqs. 5, 10) provided that the Mo:Fe ratio  
8  
9 is ~1:1. For the H304 mutants the ICP analyses (Table S1) showed that the Mo to Fe  
10  
11 ratio was ~0.6; therefore, meaningful Mo potentials could not be calculated for these  
12  
13 mutants. However, for the R309 mutants the Mo to Fe ratios determined by ICP (Table  
14  
15 S1) were sufficiently large that the IET equilibrium constants could be used to calculate  
16  
17 the Mo(VI/V) potentials (Table 2). None of the R309 mutations dramatically changed the  
18  
19 Mo potential as compared to wt (Table 2). Thus, although the heme midpoint potentials  
20  
21 for R309M and R309K are significantly lower than wt, the fact that the  $K_{eq}$  values are  
22  
23 shifted to a value closer to one, reflects the smaller driving force between Fe and Mo for  
24  
25 these two mutants.  
26  
27  
28  
29  
30

### 31 **Fatal mutation R309H**

32  
33  
34 Several fatal point mutations have been identified in patients diagnosed  
35  
36 with sulfite oxidase deficiency, including R309H (10). This work shows that purified  
37  
38 R309H hSO has substantially *increased* catalytic activity (~3-fold greater than wt) and a  
39  
40 slightly less efficient  $K_m$  sulfite. At pH 7.6,  $k_{et}$  is ~2  $k_{turnover}$ , so as noted above, IET 2 is  
41  
42 not rate limiting. This mutation gave small positive changes in the midpoint potentials  
43  
44 (Table 2) of the heme (+7 mV) and Mo (+11 mV) that are marginally significant.  
45  
46  
47

48  
49 Unlike other fatal hSO mutations that have been studied (22, 25, 26), the data for  
50  
51 purified R309H do not reveal any obvious reasons for this mutation causing sulfite  
52  
53 oxidase deficiency. The midpoint potentials of Fe and Mo are somewhat increased,  
54  
55  $K_m^{sulfite}$  is slightly increased, the activity is increased, and the enzyme still shows IET,  
56  
57  
58  
59  
60

1  
2  
3 although the rates are slow compared to wt. It is possible that these combined slight  
4  
5 changes of the properties of the protein could cause SO deficiency; however, attractive  
6  
7 alternative explanations are that this mutation causes structural instability or expression  
8  
9 problems *in vivo*.  
10  
11

## 12 Conclusions

13  
14  
15 The catalytic cycle of Figure 1 has been the standard model for describing  
16  
17 and analyzing the mechanism of vertebrate SOs, including hSO, for over 30 years (1, 4).  
18  
19 The catalytic mechanism of SO includes two redox active metals (Mo(VI/V/IV) and  
20  
21 Fe(III/II)), and two substrates (sulfite and cyt *c*). A previous detailed kinetic study of  
22  
23 native chicken SO (cSO) investigated the steady-state reduction of sulfite by cyt *c*, as  
24  
25 well as the kinetics of the rapid reduction of cSO by sulfite in the absence of cyt *c* (29).  
26  
27 The rapid two-electron reduction by sulfite generated substantial amounts of the  
28  
29 Fe(II)/Mo(V) state of SO (Figure 1), consistent with microcoulometric studies of cSO  
30  
31 which yield a driving force of ~300 mV for the IET 1 process (39). The reaction of  
32  
33 oxidized SO with excess sulfite is also an efficient method for generating the Mo(V) state  
34  
35 for detailed structural studies by pulsed EPR spectroscopy (41).  
36  
37  
38  
39

40  
41 The proposed oxidative half-reaction of hSO (left side of Figure 1) involves two  
42  
43 one-electron *intermolecular* steps with an intervening *intramolecular* electron transfer  
44  
45 reaction (IET 2). The one-electron reduced Fe(II)/Mo(VI) state of hSO can be produced  
46  
47 directly in the absence of substrates by laser flash photolysis, and the kinetics of  
48  
49 *intramolecular* electron transfer (IET 2) followed spectrophotometrically (Figure 5) (38).  
50  
51 In spite of the small driving force for the IET 2 reaction (39, 17) and the 32 Å distance  
52  
53 between Fe and Mo in the cSO crystal structure (11),  $k_{\text{et}}$  is much larger than  $k_{\text{turnover}}$  for wt  
54  
55  
56  
57  
58  
59  
60



1  
2  
3  
4  
5  
6  
7  
8  
9  
10  
11  
12  
13  
14  
15  
16  
17  
18  
19  
20  
21  
22  
23  
24  
25  
26  
27  
28  
29  
30  
31  
32  
33  
34  
35  
36  
37  
38  
39  
40  
41  
42  
43  
44  
45  
46  
47  
48  
49  
50  
51  
52  
53  
54

cSO and hSO. This observation led to the proposal that facile interdomain motion of the Fe(II)/Mo(VI) state decreases the Fe...Mo distance and facilitates rapid intramolecular electron transfer (IET 2) (13). The kinetic and thermodynamic properties of numerous mutants of recombinant hSO have been investigated to gain additional insight into the proposed overall mechanism of hSO (Figure 1), the interdomain motion model for IET 2, and clues why certain mutations cause isolated sulfite oxidase deficiency. The present work shows that the H304 and R309 mutants of hSO all have *smaller*  $k_{et}$  values than wt hSO, but that their  $k_{cat}$  values are *greater* than wt hSO. However, in nearly all cases the value of  $k_{et}$  is substantially greater than  $k_{turnover} = 1/2k_{cat}$  (see Table S3). Even the R309E mutant that reverses the charge at residue 309 from positive to negative, has  $k_{turnover} < k_{et}$ . Thus, for these H304 and R309 mutants, as with wt hSO, IET 2 is not the rate limiting step. In contrast, several catalytically competent mutants of R472 (42) and of aromatic surface residues of the Mo domain (18) show greatly impaired IET 2 ( $k_{et} \ll k_{turnover}$ ). Clearly, crystal structures of some of these mutants of hSO are important for understanding their detailed conformations and properties. However, to date only one crystal structure of an *intact* SO protein is available, that of native cSO (11), and recombinant hSO proteins have proven to be unusually difficult to crystallize in their intact form. Theoretical studies of the dynamics of interdomain motion have begun to appear (15, 16) that corroborate the proposal from the viscosity dependence of the rate of IET 2 for wt SO (14), but direct experimental measurements of the proposed interdomain dynamics are not yet available. Thus, complete unraveling of the intimate mechanism of hSO and the reasons that certain mutations are fatal remains an unresolved challenge.

55  
56  
57  
58  
59  
60

Finally, the kinetic and spectroscopic properties of a purified mutant protein may

1  
2  
3 not indicate why the particular mutation is fatal *in vivo*. For example, although the exact  
4  
5 role of the phosphate group of Moco in hSO is not known, the surrounding network of  
6  
7 hydrogen bonding residues could possibly protect the cofactor from degradation by the  
8  
9 action of phosphatases within the cell. *In vitro* studies of purified mutant proteins  
10  
11 eliminate interactions with other enzymes and bioactive molecules, and under such  
12  
13 conditions some hSO mutants might exhibit enhanced steady-state activity.  
14  
15  
16  
17  
18  
19

### 20 **Acknowledgements**

21  
22 Support of this research by the National Institute of General Medical Sciences is  
23  
24 gratefully acknowledged (Grant GM-37773 to JHE; Ruth L. Kirchstein-NIH  
25  
26 Fellowship1F32GM082136-01 to KJW). We thank Dr. K. V. Rajagopalan for providing  
27  
28 the pTG918 plasmid containing the hSO gene used to prepare the recombinant hSO  
29  
30 enzyme. We thank Dr. F. Ann Walker for the use of equipment and Dr. R. E. Berry for  
31  
32 helpful discussions. A.C.D. was a participant in the Undergraduate Biology Research  
33  
34 Program and was supported in part by a grant to the University of Arizona from the  
35  
36 Howard Hughes Medical Institute (52003749).  
37  
38  
39  
40  
41  
42  
43  
44  
45  
46  
47  
48  
49  
50  
51  
52  
53  
54  
55  
56  
57  
58  
59  
60

## Figures

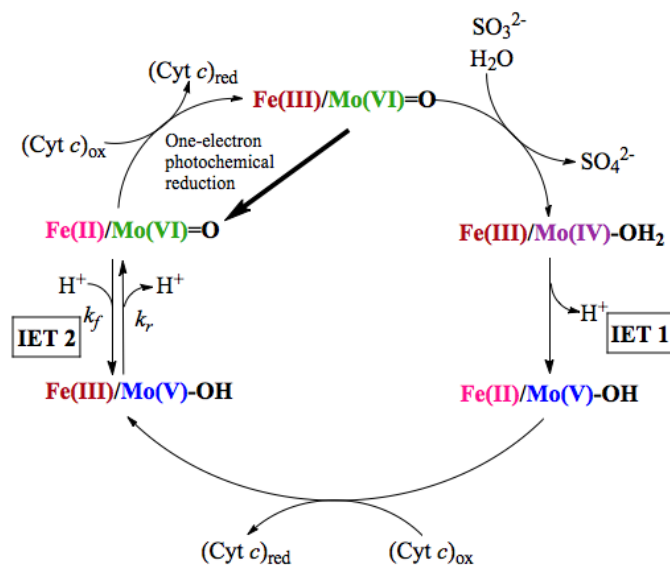


**Figure 1.** Proposed oxidation state changes occurring at the Mo and Fe centers of one subunit of hSO during the catalytic oxidation of sulfite and the concomitant reduction of (cyt *c*)<sub>ox</sub>. Only the equatorial oxygen atom among the ligands of Mo is shown for clarity. The one-electron photochemical reduction of Fe(III), indicated by the solid dark arrow, generates the Fe(II)/Mo(VI) state which undergoes IET 2. The directions of  $k_f$  and  $k_r$  refer to the flash photolysis experiment. Adapted from (19).

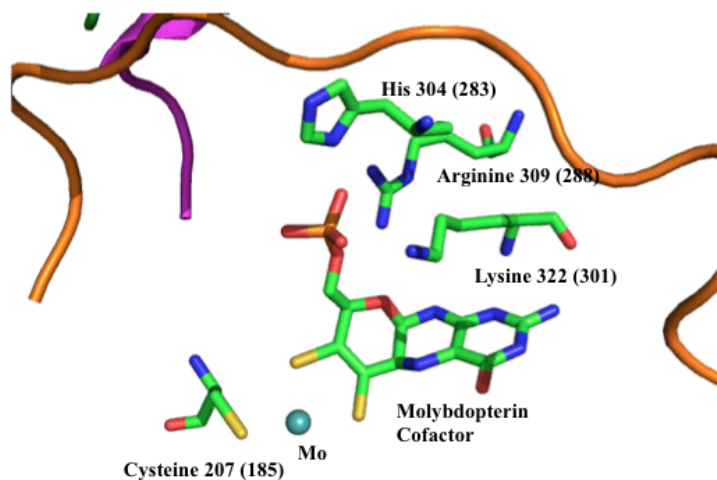


**Figure 2.** Crystal structure of cSO<sup>11</sup> (pdb 1SOX) showing H304, R309, K322, C207 and the molybdenum cofactor. Numbering reflects hSO, while cSO numbering is shown in parenthesis.

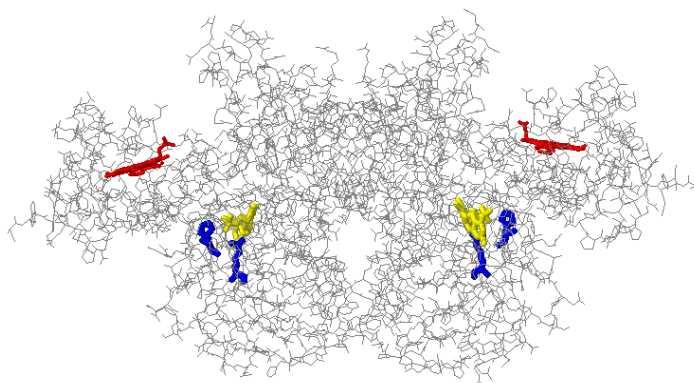


**Figure 3.** Crystal structure of cSO<sup>11</sup> (pdb 1SOX). Heme shown in red, Moco shown in yellow, and residues that have been mutated in hSO are in blue.

1  
2  
3  
4  
5  
6  
7  
8  
9  
10  
11  
12  
13  
14  
15  
16  
17  
18  
19  
20  
21  
22  
23  
24  
25  
26  
27  
28  
29  
30  
31  
32  
33  
34  
35  
36  
37  
38  
39  
40  
41  
42  
43  
44  
45  
46  
47  
48  
49  
50  
51  
52  
53  
54  
55  
56  
57  
58  
59  
60

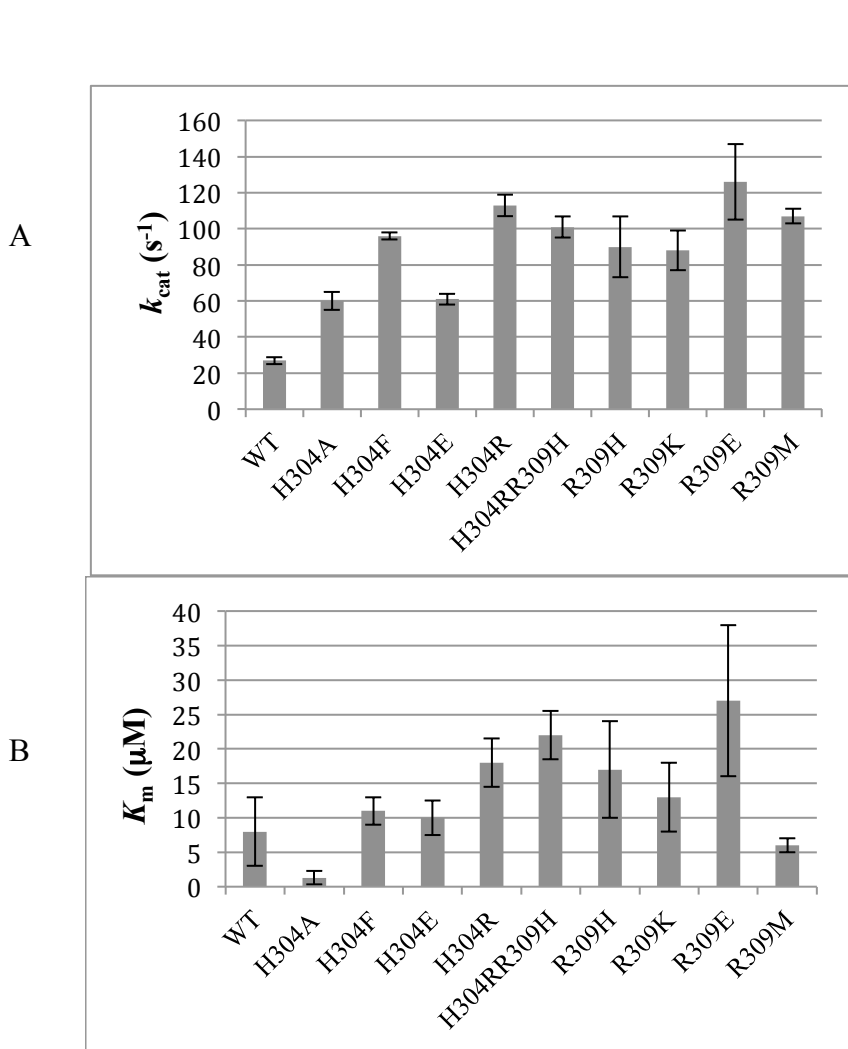


**Figure 4.** The  $k_{\text{cat}}$  (A) and  $K_m$  (B) values for H304 and R309 mutants compared to wt hSO, measured using 20 mM Tris Acetate, pH 7.6

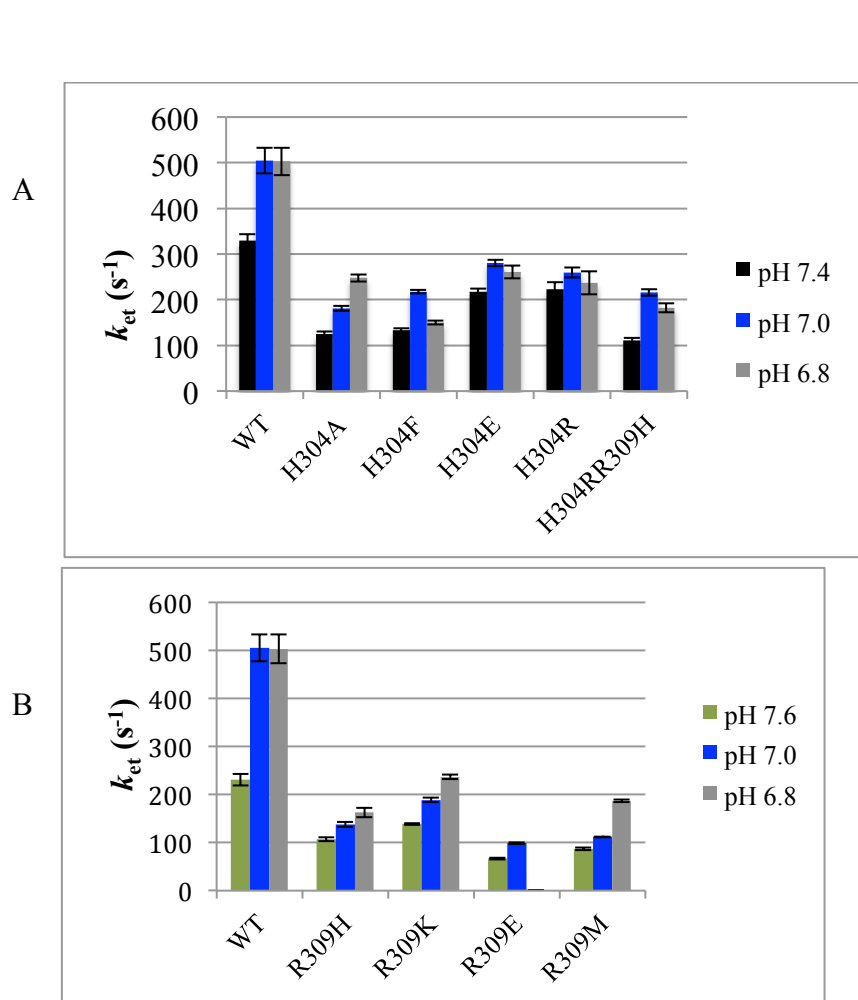


**Figure 5.** IET rates ( $k_{\text{et}}$  ( $\text{s}^{-1}$ )) for the H304 (A) and R309 (B) mutants, measured using 20 mM Tris Acetate.

**Table 1.** The Fe midpoint potentials of H304 mutants versus wt hSO, measured using 20 mM Tris Acetate at pH 7.4

	Fe midpoint potential (mV vs SHE)
<b>wt</b>	<b>54 ± 2</b>
H304F	43 ± 2
H304E	56 ± 2
H304R	51 ± 2
H304R/R309H	52 ± 2



**Table 2.** The Fe midpoint potentials, IET  $K_{eq}$  values, and calculated Mo midpoint potentials of R309 mutants versus wt hSO, measured using 20 mM Tris Acetate at pH 7.4

	Fe midpoint potential (mV vs SHE)	$K_{eq}$	Calculated Mo potential (mV vs SHE)
<b>wt</b>	<b>54 ± 2</b>	<b>0.36 ± 0.01</b>	<b>27</b>
R309H	61 ± 3	0.41 ± 0.02	38
R309K	23 ± 5	1.24 ± 0.04	29
R309M	30 ± 5	0.79 ± 0.05	24

Table of Contents Figure Only

**Kinetic Results for Mutations of Conserved Residues H304 and R309 of Human Sulfite Oxidase Point to Mechanistic Complexities**

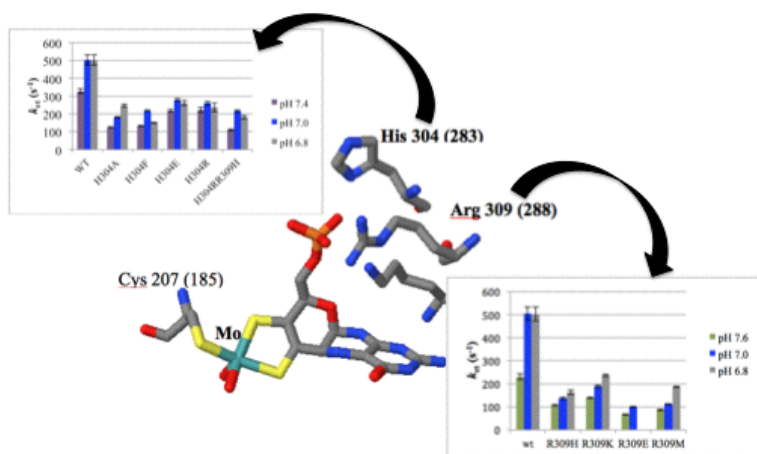
Amanda C. Davis,<sup>1</sup> Kayunta Johnson-Winters,<sup>2\*</sup> Anna R. Arnold,<sup>1</sup> Gordon Tollin,<sup>1</sup>

John H. Enemark<sup>1</sup>

<sup>1</sup>Department of Chemistry and Biochemistry, University of Arizona, Tucson, Arizona, 85721-0041

<sup>2</sup>Department of Chemistry and Biochemistry, University of Texas at Arlington, Arlington, Texas 76019-0065

\*[Kayunta@uta.edu](mailto:Kayunta@uta.edu)



## References

1. Rajagopalan, K. V., 1980, Sulfite Oxidase (Sulfite:Ferricytochrome *c* Oxidoreductase). In: Molybdenum and Molybdenum-Containing Enzymes, 1st ed.; Coughlan, M. P., Ed.; Pergamon Press, Oxford, U.K., pp. 241-272.
2. Johnson, J. L., and Rajagopalan, K. V., *J. Biol. Chem.*, 1977, **252**, 2017-2025.
3. Kessler, D. L., and Rajagopalan, K. V., *J. Biol. Chem.*, 1972, **247**, 6566-6573.
4. Hille, R., *Biochim. Biophys. Acta.*, 1994, **1184**, 143-169.
5. Cohen, H. J., Betcher-Lange, S., Kessler, D. L., and Rajagopalan, K. V., *J. Biol. Chem.*, 1972, **247**, 7759-7766.
6. Schindelin, H., Kisker, C., and Rajagopalan, K. V., *Adv. Protein. Chem.* 2001, **58**, 47-94.
7. Schwarz, G., and Mendel, R. R., *Annu. Rev. Plant Biol.*, 2006, **57**, 623-647.
8. Veldman, A., Santamaria-Araujo, J. A., Sollazzo, S., Pitt, J., Gianello, R., Yaplito-Lee, J., Wong, F., Ramsden, C. A., Reiss, J., Cook, I., Fairweather, J., and Schwarz, G., *Pediatrics* 2010, **125**, e1249-1254.
9. Rugar, C. A., Gillett, J., Gordon, B. A., Ramsay, D. A., Johnson, J. L., Garrett, R. M., Rajagopalan, K. V., Jung, J. H., Bachevie, G. S., and Sellers, A. R., *Neuropediatrics*, 1996, **27**, 299-304.

10. Johnson, J. L., Coyne, K. E., Garrett, R. M., Zobot, M. T., Dorche, C., Kisker, C., and Rajagopalan, K. V., *Hum. Mutat.*, 2002, **20**, 74.
11. Kisker, C., Schindelin, H., Pacheco, A., Wehbi, W. A., Garrett, R. M., Rajagopalan, K. V., Enemark, J. H., and Rees, D. C., 1997, *Cell* **91**, 973-983.
12. Astashkin, A. V., Rajapakshe, A., Cornelison, M. J., Johnson-Winters, K., and Enemark, J. H., *J. Phys. Chem. B*, **116**, 2012, 1942-1950.
13. Pacheco, A., Hazzard, J. T., Tollin, G., and Enemark, J. H., *J. Biol. Inorg. Chem.*, 1999, **4**, 390-401.
14. Feng, C., Kedia, R. V., Hazzard, J. T., Hurley, J. K., Tollin, G., and Enemark, J. H., *Biochemistry*, 2002, **41**, 5816-5821.
15. Pushie, M. J., and George, G. N., *J. Phys. Chem. B*, **114**, 2010, 3266-3275.
16. Utesch, T., and Mroginski, M. A., *J. Phys. Chem. Lett.* **1**, 2010, 2159-2164.
17. Johnson-Winters, K., Nordstrom, A. R., Emesh, S., Astashkin, A. V., Rajapakshe, A., Berry, R. E., Tollin, G., and Enemark, J. H., *Biochemistry*, 2010, **49**, 1290-1296.
18. Rajapakshe, A., Meyers, K. T., Berry, R. E., Tollin, G., and Enemark, J. H., *J. Biol. Inorg. Chem.*, 2012, **17**, 345-352.
19. Davis, A. C., Cornelison, M. J., Meyers, K. T., Rajapakshe, A., Berry, R. E., Tollin, G., Enemark, J. H., *Dalton Trans.*, 2013, **42**, 3043-9.
20. Wilson, H. L., and Rajagopalan, K. V., *J. Biol. Chem.*, 2004, **279**, 15105-15113.

- 1  
2  
3  
4  
5  
6  
7  
8  
9  
10  
11  
12  
13  
14  
15  
16  
17  
18  
19  
20  
21  
22  
23  
24  
25  
26  
27  
28  
29  
30  
31  
32  
33  
34  
35  
36  
37  
38  
39  
40  
41  
42  
43  
44  
45  
46  
47  
48  
49  
50  
51  
52  
53  
54  
55  
56  
57  
58  
59  
60
21. Feng, C., Wilson, H. L., Hurley, J. K., Hazzard, J. T., Tollin, G., Rajagopalan, K. V., and Enemark, J. H., *J. Biol. Chem.*, 2003, **278**, 2913-2920.
  22. Feng, C., Wilson, H. L., Hurley, J. K., Hazzard, J. T., Tollin, G., Rajagopalan, K. V., and Enemark, J. H., *Biochemistry*, 2003, **42**, 12235-12242.
  23. Feng, C., Wilson, H. L., Tollin, G., Astashkin, A. V., Hazzard, J. T., Rajagopalan, K. V., and Enemark, J. H., *Biochemistry*, 2005, **44**, 13734-13743.
  24. Astashkin, A. V., Johnson-Winters, K., Klein, E. L., Feng, C., Wilson, H. L., Rajagopalan, K. V., Raitsimring, A. M., and Enemark, J. H., 2008, *J. Am. Chem. Soc.* **130**, 8471-8480.
  25. Rajapakshe, A., Tollin, G., and Enemark, J. H., 2012, *Chem. Biodiversity* **9**, 1621-1634. doi:10.1002/cbdv.201200010
  26. Emesh, S., Rapson, T. D., Rajapakshe, A., Kappler, U., Bernhardt, P. V., Tollin, G., and Enemark, J. H., *Biochemistry*, 2009, **48**, 2156-2163.
  27. Temple, C. A., Graf, T. N., and Rajagopalan, K. V., *Arch. Biochem. Biophys.*, 2000, **383**, 281-287.
  28. Garrett, R. M., and Rajagopalan, K. V., *J. Biol. Chem.*, 1996, **271**, 7387-7391.
  29. Brody, M. S., and Hille, R., *Biochemistry*, 1999, **38**, 6668-6677.
  30. Kipke, C. A., Cusanovich, M. A., Tollin, G., Sunde, R. A., and Enemark, J. H., *Biochemistry*, 1988, **27**, 2918-2926.

- 1  
2  
3  
4  
5  
6  
7  
8  
9  
10  
11  
12  
13  
14  
15  
16  
17  
18  
19  
20  
21  
22  
23  
24  
25  
26  
27  
28  
29  
30  
31  
32  
33  
34  
35  
36  
37  
38  
39  
40  
41  
42  
43  
44  
45  
46  
47  
48  
49  
50  
51  
52  
53  
54  
55  
56  
57  
58  
59  
60
31. Hurley, J. K., Weber-Main, A. M., Stankovich, M. T., Benning, M. M., Thoden, J. B., Vanhooke, J. L., Holden, H. M., Chae, Y. K., Xia, B., Cheng, H., Markley, J. L., Martinez-Julvez, M., Gomez-Moreno, C., Schmeits, J. L., and Tollin, G., *Biochemistry*, 1997, **36**, 11100-11117.
32. Tollin, G., 2008, Interprotein and Intraprotein Electron Transfer Mechanisms, In: *Electron Transfer in Chemistry*, Balzani, V., Ed.; Wiley-VCH Verlag GmbH, Weinheim, Germany, Vol. IV, pp 202-231.
33. Tollin, G., *J. Bioenerg. Biomembr.* 1995, **27**, 303-309.
34. Tollin, G., Hurley, J. K., Hazzard, J. T., and Meyer, T. E., *Biophys. Chem.* 1993, **48**, 259-279.
35. Berry, R. E., Shokhireva, T., Filippov, I., Shokhirev, M. N., Zhang, H., and Walker, F. A., *Biochemistry*, 2007, **46**, 6830-6843.
36. Ding, X. D., Weichsel, A., Andersen, J. F., Shokhireva, T. K., Balfour, C., Pierik, A. J., Averill, B. A., Montfort, W. R., and Walker, F. A., *J. Am. Chem. Soc.*, 1999, **121**, 128-138.
37. Hellwig, P., Behr, J., Ostermeier, C., Richter, O. M., Pfitzner, U., Odenwald, A., Ludwig, B., Michel, H., and Mantele, W., *Biochemistry*, 1998, **37**, 7390-7399.
38. Feng, C., Tollin, G., and Enemark, J. H., *Biochim. Biophys. Acta.* 2007, **1774**, 527-539.
39. Spence, J. T., Kipke, C. A., Enemark, J. H., and Sunde, R. A., *Inorg. Chem.*, 1991, **30**, 3011-3015.
40. Kappler, U., and Bailey, S., *J. Biol. Chem.*, 2005, **280**, 24999-25007.

- 1  
2  
3  
4  
5  
6  
7  
8  
9  
10  
11  
12  
13  
14  
15  
16  
17  
18  
19  
20  
21  
22  
23  
24  
25  
26  
27  
28  
29  
30  
31  
32  
33  
34  
35  
36  
37  
38  
39  
40  
41  
42  
43  
44  
45  
46  
47  
48  
49  
50  
51  
52  
53  
54  
55  
56  
57  
58  
59  
60
41. Klein, E. L., Astashkin, A. V., Raitsimring, A. M., Enemark, J. H., *Coord. Chem. Rev.*, **2013**, **257**, 110–118.
42. Johnson-Winters, K., Davis, A. C., Arnold, A. R., Berry, R. E., Tollin, G., Enemark, J. H., *J. Biol. Inorg. Chem.* **2013**, *18*, 645-653.